

# Analyst

Accepted Manuscript



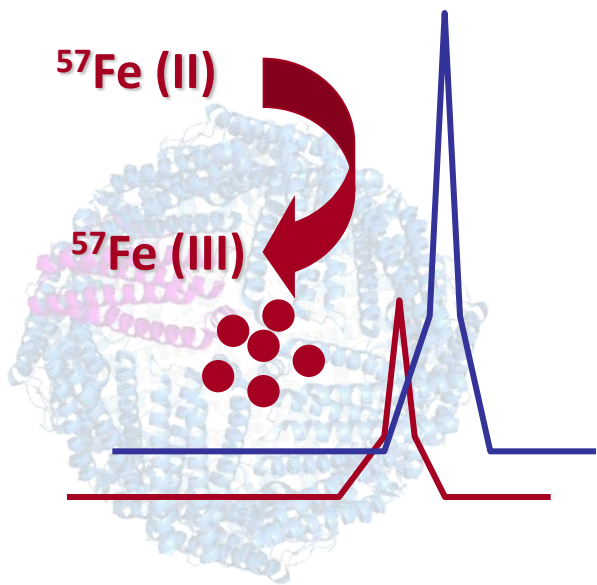
This is an *Accepted Manuscript*, which has been through the Royal Society of Chemistry peer review process and has been accepted for publication.

*Accepted Manuscripts* are published online shortly after acceptance, before technical editing, formatting and proof reading. Using this free service, authors can make their results available to the community, in citable form, before we publish the edited article. We will replace this *Accepted Manuscript* with the edited and formatted *Advance Article* as soon as it is available.

You can find more information about *Accepted Manuscripts* in the [Information for Authors](#).

Please note that technical editing may introduce minor changes to the text and/or graphics, which may alter content. The journal's standard [Terms & Conditions](#) and the [Ethical guidelines](#) still apply. In no event shall the Royal Society of Chemistry be held responsible for any errors or omissions in this *Accepted Manuscript* or any consequences arising from the use of any information it contains.

1  
2  
3  
4  
5  
6  
7  
8  
9  
10  
11  
12  
13  
14  
15  
16  
17  
18  
19  
20  
21  
22  
23  
24  
25  
26  
27  
28  
29  
30  
31  
32  
33  
34  
35  
36  
37  
38  
39  
40  
41  
42  
43



1  
2  
3  
4  
5  
6  
7  
8  
9  
10  
11  
12  
13  
14  
15  
16  
17  
18  
19  
20  
21  
22  
23 **INCORPORATION OF ISOTOPICALLY ENRICHED  $^{57}\text{Fe}$  IN APOFERRITIN:**  
24 **FORMATION AND CHARACTERIZATION OF ISOTOPICALLY ENRICHED**  
25 **Fe NANOPARTICLES FOR METABOLIC STUDIES.**  
26  
27  
28

29  
30 T. Konz, M. Montes-Bayón\* and A. Sanz-Medel\*  
31

32  
33 Department of Physical and Analytical Chemistry. Faculty of Chemistry. University of  
34

35  
36 Oviedo. C/Julián Clavería 8, 33006 Oviedo. Spain.  
37

38  
39 [montesmaria@uniovi.es](mailto:montesmaria@uniovi.es), [asm@uniovi.es](mailto:asm@uniovi.es)  
40  
41  
42  
43  
44  
45  
46  
47  
48  
49  
50  
51  
52  
53  
54  
55  
56  
57  
58  
59  
60

**ABSTRACT**

The use of  $^{57}\text{Fe}$ -isotopically enriched ferritin for the accurate measurement of Fe:ferritin ratios is proposed for metabolic studies. Thus, the synthesis of  $^{57}\text{Fe}$ -isotopically enriched ferritin from horse apo-ferritin and isotopically enriched  $(\text{NH}_4)_2^{57}\text{Fe}(\text{II})(\text{SO}_4)_2$  (Mohr's salt) is conducted. Size exclusion chromatography on-line with UV-VIS absorption (at 380 nm) is used in order to monitor the loading process of apo-ferritin. These studies revealed that the Fe-incorporation process involves also the formation of protein aggregates (oligomers) showing higher molecular mass than ferritin. A final optimized protocol involving incubation of the synthesized standard with guanidine hydrochloride (pH 3.5) has provided the best conditions for maintaining as stable protein structure without aggregates. Such  $^{57}\text{Fe}$ -isotopically enriched ferritin was characterized and contained as average 2200 atoms of Fe/mol ferritin. The evaluation of the Fe-core after saturation with  $^{57}\text{Fe}$  by Transmission Electron Microscopy (TEM) has revealed the formation of  $^{57}\text{Fe}$  nanoparticles with a similar diameter to this of the commercial Fe-containing ferritin, confirming the process of Fe uptake, oxidation and mineralization within the protein cavity. The synthesized  $^{57}\text{Fe}$ -ferritin shows a great potential as nanometabolic tracer to study the kinetics of Fe release in cases of iron metabolic disorders.

**Key-words:** ferritin, isotopically enriched, ICP-MS, oligomers, nanoparticles.

## Introduction

Iron is an essential micronutrient that is required for an adequate erythropoietic function, oxidative metabolism and cellular immune response.<sup>1</sup> Absorption of dietary iron (1-2 mg/day) is tightly regulated, and just balanced with losses, because there is no active mechanism of iron excretion.<sup>2</sup> The measurement of iron imbalances in the organisms include a number of parameters related to the main iron transporting protein in plasma, transferrin (Tf).<sup>3</sup> Among them, the Tf-saturation level (amount of Fe associated to Tf binding sites) or serum iron are commonly monitored in clinical labs.<sup>4,5</sup> In addition to Tf-related parameters, ferritin is the other key biomarker in Fe metabolism.<sup>6,7</sup> Actually, the measurement of ferritin provides the most useful indirect estimate of body iron stores.<sup>8</sup>

Ferritin is a 440 kDa protein composed by 24 subunits that form a hollow protein shell holding inside an internal cavity of about 8 nm internal diameter that can contain a variable amount of iron atoms (up to 4500) by forming a so-called biological nanoparticles.<sup>9,10</sup> The 24 polypeptide subunits do not have the same structure neither function. While the H-chain (21 kDa) shows catalytic ferroxidase activity and is responsible for the oxidation of Fe (II) to Fe (III), the L-subunit (19 kDa) is associated with iron nucleation, mineralization and long-term iron storage within the ferritin cavity mainly in the form of Fe<sub>2</sub>O<sub>3</sub> nanoparticles (NPs).<sup>11</sup> The chains H/L ratio varies among tissues and therefore, the number of Fe atoms stored into the internal cavity of ferritin is not constant either.<sup>12</sup> In fact, the Fe load of ferritin has been proposed by some authors as a more specific biomarker of Fe-homeostasis disorders than the measurement of only the protein shell. Nowadays, ferritin (and its Fe content) is increasingly being recognized as a crucial molecule in some neurological pathologies such as Parkinson (PD) or Alzheimer's (AD) diseases. In PD patients a marked reduction of the ferritin expression in the brain as well

1  
2  
3 as the alteration of neuromelanin structure seems to compromise the iron sequestration  
4 capabilities leading to the accumulation of free metal ion. Thus, understanding the  
5 chemical structure of the ferritin core may help to elucidate the alteration or dysfunction  
6 of ferritin and its role in the development of degenerative diseases. This includes the  
7 ferritin iron uptake, storage, and release mechanisms in detail in order to understand the  
8 etiologic origin of some of these syndromes.<sup>13,14</sup>  
9  
10  
11  
12  
13  
14  
15

16  
17 For the aim of studying Fe-ferritin related parameters an interesting possibility is  
18 the use of <sup>57</sup>Fe isotopically enriched ferritin. Using a non-toxic isotopic label is especially  
19 favourable to investigate, among others, whether serum ferritin losses most of its Fe during  
20 or after effluxing from the cells in which it originates.<sup>15</sup> The synthesis and characterization  
21 of <sup>57</sup>Fe-ferritin has been attempted before by biochemical heterologous expression in *E.*  
22 *coli* in the presence of <sup>57</sup>Fe.<sup>16,17</sup> In that case, the expressed protein was the plant ferritin  
23 (different to the human species) and the production yield turned out to be relatively low.  
24 In this work, this challenging task has been accomplished by chemical synthesis using  
25 apo-ferritin from horse spleen that was then enriched in <sup>57</sup>Fe using isotopically enriched  
26 (NH<sub>4</sub>)<sub>2</sub><sup>57</sup>Fe(II)(SO<sub>4</sub>)<sub>2</sub> (Mohr's salt), as the source of enriched Fe (II) previously  
27 synthesized. Different salts have been used in previous experiments for Fe-loading into  
28 apoferritin including FeSO<sub>4</sub> or (NH<sub>4</sub>)<sub>2</sub>Fe(SO<sub>4</sub>)<sub>2</sub>. This double sulphate (Mohr's salt) has  
29 been chosen since the Fe(II) present in the compound is less prone to be oxidized by the  
30 dissolved oxygen than other Fe(II) salts. The oxidation of Fe (II) is very pH dependent,  
31 occurring much more readily at high pH. The ammonium ions make solutions of Mohr's  
32 salt slightly acidic, which slows this oxidation process. Both, the <sup>57</sup>Fe incorporation  
33 kinetics and the stability of the synthesized metalloprotein have been carefully evaluated  
34 here. The final isotopically enriched protein has been quantitatively characterized for the  
35 metal (Fe) and the protein (S) using SEC-ICP-MS and post-column isotope dilution of  
36  
37  
38  
39  
40  
41  
42  
43  
44  
45  
46  
47  
48  
49  
50  
51  
52  
53  
54  
55  
56  
57  
58  
59  
60

1  
2  
3 sulphur and of iron (using enriched  $^{34}\text{S}$  to address the protein content and reversed IDA  
4  
5 with natural Fe to address the incorporated  $^{57}\text{Fe}$  respectively).  
6  
7

8 The complementary information provided by TEM (monitoring the formation of  
9  
10 iron NPs from isotopically enriched  $^{57}\text{Fe}$ ) together with the information obtained by SEC-  
11  
12 ICP-MS (in terms of Fe isotope ratios and Fe/S measurements) has permitted to fully  
13  
14 characterize the synthesized nanometabolic tracer  $^{57}\text{Fe}$ -ferritin that shows an extraordinary  
15  
16 potential to address Fe/ferritin ratios in biological samples as well as kinetics studies on  
17  
18 the iron mobilization mechanisms (e.g. in Alzheimer's disease).  
19  
20  
21

## 22 **Materials and Methods**

### 23 **Instrumentation.**

24  
25  
26 All ICP-MS experiments during this study were performed using a Thermo Element 2  
27  
28 (Thermo Fisher Scientific, Bremen, Germany) mass spectrometer, equipped with a double  
29  
30 focusing sector field mass analyzer applying medium resolution ( $m/\Delta m=4000$ ) both for Fe  
31  
32 and S detection. The observed optimized parameters for Fe and S of the Element 2  
33  
34 instrument are summarized in Table 1. The ICP-MS instrument was fitted with a  
35  
36 concentric nebulizer and a Scott double-pass spray chamber. For the final evaluation of  
37  
38 ferritin purity, after its isolation from other serum components, we used size exclusion  
39  
40 chromatography (SEC). The HPLC separation was carried out using a dual-piston liquid  
41  
42 chromatographic pump (Shimadzu LC-20AD, Shimadzu Corporation, Kyoto, Japan)  
43  
44 equipped with a sample injection valve from Rheodyne, fitted with a 100  $\mu\text{L}$  injection  
45  
46 loop and a size exclusion chromatography column Superdex 200 10/300 GL (300 mm x  
47  
48 10 mm i.d., GE Healthcare Bio-Sciences, Sweden). The mobile phase flow was 0.75  
49  
50 mL/min and the absorbance of the ferritin was monitored at 280 and 380 nm (specific of  
51  
52  
53  
54  
55  
56  
57  
58  
59  
60

1  
2  
3 the iron-protein complex) using a Diode Array Detector (DAD) detector (Agilent  
4  
5 Technologies, Waldbronn, Germany).  
6  
7

8 For evaluation of isotopic abundances of the  $^{57}\text{Fe}$ -ferritin, the size exclusion  
9  
10 column was coupled on-line with multicollector (MC)-ICP-MS (Neptune, Thermo Fisher  
11  
12 Scientific). The Neptune MC-ICP-MS is equipped with eight adjustable Faraday cups, one  
13  
14 fixed central cup, and a secondary electron multiplier. To increase the sensitivity, the  
15  
16 instrument is also equipped with a guard electrode that improves the ion-transmission  
17  
18 efficiency and prevents formation of secondary discharges. Iron isotope ratio  
19  
20 measurements were performed using the medium resolution setting of the entrance slit.  
21  
22 The system configuration for Fe measurements is similar to the one described in the  
23  
24 literature.<sup>18</sup>  
25  
26  
27  
28

29 TEM measurements were done in a JEOL-JEM 2100F (200 kV) transmission  
30  
31 electron microscope to image ferritin solutions deposited on Cu grids. The instrument  
32  
33 permits also to obtain the elemental composition of the sample.  
34  
35  
36

### 37 **Chemicals and materials**

38  
39 All solutions were prepared using  $18\text{ M}\Omega\text{ cm}^{-1}$  de-ionized water obtained from a Milli-Q  
40  
41 system (Millipore, Bedford, MA, USA). Ferritin standards from equine spleen (apo and  
42  
43 Fe-containing), human spleen and human liver were purchased from Sigma-Aldrich (St.  
44  
45 Louis, MO, USA). Isotopically enriched  $^{34}\text{S}$  (abundances:  $^{34}\text{S}$  99.91%,  $^{32}\text{S}$  0.09%) used  
46  
47 for ICP-MS protein quantification by IDA was purchased from Euriso-top (Saint-Aubin  
48  
49 Cedex, France). Isotopically enriched elemental iron with relative abundances 0.043%  
50  
51  $^{54}\text{Fe}$ , 4.96%  $^{56}\text{Fe}$ , 94.52%  $^{57}\text{Fe}$ , 0.47%  $^{58}\text{Fe}$  was obtained from Spectrascan (Teknolab A.S.  
52  
53 Dröbak, Norway). The synthesis of Mohr's salt  $(\text{NH}_4)_2^{57}\text{Fe}(\text{II})(\text{SO}_4)_2$  from the solid is  
54  
55 detailed in the procedures section.  
56  
57  
58  
59  
60



1  
2  
3 The mobile phase for SEC separation of ferritin synthesis products was 50 mM  
4 ammonium acetate (pH 7.4) from Sigma Aldrich. For decreasing oligomers formation  
5 during the synthesis of isotopically enriched ferritin, solutions containing 0.06 M  
6 dithiothreitol (DTT) or 7 M guanidinium hydrochloride were prepared from the  
7 corresponding solid compounds obtained from Sigma. Concentrated H<sub>2</sub>SO<sub>4</sub> and  
8 (NH<sub>4</sub>)<sub>2</sub>SO<sub>4</sub> were purchased by Merck (Merck, Darmstadt, Germany) and HEPES from  
9 Sigma Aldrich.  
10  
11  
12  
13  
14  
15  
16  
17  
18

### 19 **Synthesis of <sup>57</sup>Fe enriched Mohr's salt.**

20  
21  
22 The suitability of the synthesis procedure was first evaluated with natural Fe (II) and then,  
23 scaled down to be applied to the more expensive isotopically enriched <sup>57</sup>Fe (II) in the more  
24 stable form of ammonium iron (II) sulphate. For the synthesis of ammonium iron (II)  
25 sulfate (Mohr's salt), 50 mg (0.9 mmol) of elemental <sup>57</sup>Fe and 0.9 mL of 1 M H<sub>2</sub>SO<sub>4</sub> were  
26 placed in a glass vial. The vial was sealed with a septum and the mixture allowed to stand  
27 overnight so that iron was completely dissolved. Separately, 118 mg (0.9 mmol) of  
28 (NH<sub>4</sub>)<sub>2</sub>SO<sub>4</sub> were dissolved in 140 μL water. Both solutions were simultaneously  
29 pre-concentrated by evaporation using a hot plate. Immediately, after an initial  
30 crystallization was observed, both solutions were mixed together by using a syringe. The  
31 reaction mixture was allowed to stand at 4°C overnight. The light green crystals were  
32 collected by vacuum filtration and washed with a few μLs ice cold water. Typically, a  
33 yield of 60% was obtained. For the characterization of the final product, the measurement  
34 of the melting point as well as the X-ray diffraction spectra were used (see supporting  
35 information).  
36  
37  
38  
39  
40  
41  
42  
43  
44  
45  
46  
47  
48  
49  
50  
51  
52

### 53 **Synthesis of <sup>57</sup>Fe-ferritin from Mohr's salt and apoferritin.**

54  
55  
56  
57  
58  
59  
60

1  
2  
3 The loading of apo-ferritin with  $(\text{NH}_4)_2^{57}\text{Fe}(\text{II})(\text{SO}_4)_2$  was achieved by a modified  
4  
5 protocol of the previously used by De Silva et al.<sup>19</sup> In brief, apo-ferritin was diluted in 50  
6  
7 mM HEPES buffer (pH 7.0) to give 4 ml of a 1  $\mu\text{M}$  solution. Additionally, the incubation  
8  
9 solution was prepared by dissolving 8 mg of ammonium iron (II) sulfate in 500  $\mu\text{L}$   
10  
11 MilliQ-water to give a concentration of 40 mM. Apo-ferritin loading was achieved by  
12  
13 adding 250  $\mu\text{L}$  of the incubation solution to the 1 $\mu\text{M}$  apo-ferritin solution (final Fe  
14  
15 concentration approx. 2500  $\mu\text{M}$ ). The reaction mixture was allowed to stand for 30 min at  
16  
17 room temperature. For the evaluation of the incorporation kinetics using  
18  
19  $(\text{NH}_4)_2^{57}\text{Fe}(\text{II})(\text{SO}_4)_2$  as Fe(II) source, the absorbance of the Fe-protein complex was  
20  
21 monitored at 380 nm using 1  $\mu\text{M}$  apo-ferritin (fixed concentration) and concentrations of  
22  
23 Fe (II) ranging from 0 to 10 mM. The absorbance was registered at different time  
24  
25 intervals from 0 to 30 min.  
26  
27  
28  
29

30  
31 To study the possible oligomerization events, after 30 minutes of incubation the  
32  
33 solution was passed through a membrane filter with a 10 kDa cut-off to remove the Fe(II)  
34  
35 excess (5000 g, 45 min, 4 °C) and the protein was washed several times with buffer 50  
36  
37 mM HEPES (pH 7). The product was then diluted in the mobile phase (50mM ammonium  
38  
39 acetate) and chromatographically analysed to address its the evolution with time (1 h, 2 h,  
40  
41 3 h, 7 d and 14 d) in absence of Fe and oxygen ( $\text{N}_2$  was applied for degassing of the  
42  
43 solution).  
44  
45

46  
47 For final cleavage of ferritin dimers and trimers, 1% DTT and 7 M guanidinium  
48  
49 chloride were evaluated, as recommended elsewhere.<sup>20</sup> Optimum results were obtained by  
50  
51 incubation of the residue obtained after ultracentrifugation with 4 ml of 7 M guanidinium  
52  
53 chloride for 45 min. For further elimination of the guanidinium chloride, the mixture was  
54  
55 ultrafiltrated again by using 10 kDa filters and washed twice with 50 mM HEPES buffer.  
56  
57 The filter residue was finally dissolved in 4 mL 50 mM ammonium acetate. Aliquots were  
58  
59  
60

1  
2  
3 stored at 4°C. The purity of the ferritin solution was confirmed by size exclusion  
4 chromatography (SEC) and UV/Vis detection.  
5  
6  
7

### 8 **Quantification strategies used by isotope dilution analysis (IDA)**

9

10  
11 Quantitative analysis of the synthesized  $^{57}\text{Fe}$ -ferritin was done by post-column isotope  
12 dilution using natural Fe and isotopically enriched  $^{34}\text{S}$  simultaneously.<sup>21-23</sup> Ferritin  
13 recoveries through the SEC column were calculated to be 85% by Fe measurements. The  
14 accuracy of the determination of S by post-column IDA in the ferritin peak (as the mean  
15 to address the protein concentration) was validated by analysing a set of human liver  
16 commercial ferritin standards by this method and comparing results with a clinically used  
17 Ru-labelling immunoassay, as developed in previous studies.<sup>24</sup>  
18  
19  
20  
21  
22  
23  
24  
25  
26  
27

28 For quantification using species specific isotope dilution analysis, a fixed volume  
29 (100  $\mu\text{L}$ ) of the synthesized enriched  $^{57}\text{Fe}$ -ferritin tracer (diluted to 6.68  $\mu\text{g Fe/mL}$ ) was  
30 mixed with equal volumes of the corresponding ferritin standards (apo and holo, with a  
31 theoretical concentration of 3.6 and 5.06  $\mu\text{g Fe/mL}$ , respectively, according to the  
32 producer) and the mixture was injected in the SEC-ICP-MS system. These standards were  
33 quantified for total ferritin using the S content, by S post-column IDA.<sup>21</sup> By integrating  
34 the peak areas of  $^{56}\text{Fe}$  and  $^{57}\text{Fe}$  in the corresponding chromatograms and knowing the Fe  
35 concentration as well as the isotope ratio of the tracer ( $^{57}\text{Fe}$ -ferritin), the total Fe  
36 concentration in the ferritin standards could be obtained by using the isotope dilution  
37 equation.<sup>25</sup>  
38  
39  
40  
41  
42  
43  
44  
45  
46  
47  
48  
49  
50

### 51 **Quantification of ferritin-bound iron in serum samples.**

52

53  
54 Human serum samples were mixed with an adequate amount of the  $^{57}\text{Fe}$ -ferritin tracer and  
55 subsequently treated by heat precipitation, aiming at the isolation of serum ferritin. Here,  
56  
57  
58  
59  
60

1  
2  
3 2 ml of each sample were heated at 75°C for 10 min. After centrifugation (15,000 g for 30  
4  
5 min, 4°C) the ferritin-containing supernatant was subjected to analysis by SEC-HPLC  
6  
7  
8 coupled to DF-ICP-MS.  
9

## 10 **Results and discussion**

### 11 **Isotopic iron incorporation kinetics.**

12  
13  
14  
15  
16  
17 The process of iron incorporation into apo-ferritin takes place in, at least, two steps: 1)  
18 oxidation of Fe(II) catalyzed by the H-subunits and 2) translocation and storage of Fe(III)  
19 by hydrolysis and polymerization in the central cavity. According to the literature, the H-  
20 chains of the ferritin show ferroxidase activity catalyzing the conversion of Fe (II) to  
21 Fe(III) that is an initial step in the preparation of iron for storage in the protein. It has  
22 been proposed by other authors that the presence of other ferroxidases such as  
23 ceruloplasmin (a serum copper ferroxidase) promotes the incorporation of iron into  
24 apoferritin.<sup>26</sup> In this case, Fe(II) seems to bind to the catalytic sites of apoferritin (which  
25 might include carboxylate groups) initiating the oxidation process catalysed by the apo-  
26 protein. The location of these binding sites has not been determined, but suggested regions  
27 are the outer surface of the apoprotein, in the channels leading to the central cavity, or  
28 inside the central core. Figure 1 shows the Fe incorporation kinetics using Mohr's salt as  
29 a most stable source of Fe(II): the initial complex formation rate is fast while after some  
30 minutes (which differ depending on the Fe(II) concentration) the reaction rate slows down  
31 (less apo-protein is available). Such results corroborate that the Fe incorporation into  
32 ferritin occurs through a first Fe(II) oxidation step that is catalyzed by apo-ferritin.<sup>26</sup>  
33  
34  
35  
36  
37  
38  
39  
40  
41  
42  
43  
44  
45  
46  
47  
48  
49  
50  
51  
52  
53  
54  
55  
56  
57  
58  
59  
60  
60 However, once the concentration of free apo-ferritin decreases, the formation rate of Fe-  
ferritin is significantly reduced although the complex saturation is not reached even after

1  
2  
3 30 minutes of reaction time. For practical considerations, this time has been selected as  
4  
5 incubation time for further experiments.  
6  
7

8 To address the purity of the synthesized species, the reaction products were  
9  
10 chromatographically separated using size exclusion chromatography with UV/VIS  
11  
12 detection and compared with a commercial standard of Fe-containing horse spleen ferritin.  
13  
14 These chromatograms can be observed in Figure 2A and 2B respectively by monitoring  
15  
16 the signals at 280 and 380nm. These results show that the synthesis product resulted in a  
17  
18 main species absorbing at both wavelengths at approximately 11.5 mL, and with similar  
19  
20 retention time to that observed for the commercial Fe-containing horse spleen ferritin.  
21  
22 Figure 2A shows also an iron peak at about 8 mL corresponding to the void volume of the  
23  
24 column (species with higher molecular mass than the exclusion limit of the column which  
25  
26 is 1300 kDa). This particular species is also detectable in the chromatogram of Fig. 2B of  
27  
28 the commercial standard but with a significantly smaller area. A possible explanation for  
29  
30 such bigger species is the formation of ferritin dimers, trimers or even oligomers during  
31  
32 the synthesis or purification procedures. Such species absorb at the same wavelengths as  
33  
34 the monomeric form of ferritin but should behave in a different way in solution (e.g.  
35  
36 regarding ultrafiltration, antibody recognition, etc.). Therefore, the synthesis conducted in  
37  
38 this way does not provide a suitable isotopically enriched ferritin standard for further  
39  
40 robust quantitative metabolic studies. Thus, specific studies to remove or minimize the  
41  
42 formation of oligomers were undertaken.  
43  
44  
45  
46  
47  
48

#### 49 **Oligomerization studies by SEC-UV/VIS and SEC-ICP-MS**

50  
51  
52 In order to study the oligomerization of the ferritin during Fe loading, some initial studies  
53  
54 were carried out to address the evolution of the synthesis product with time. The existing  
55  
56 literature in this regard is scarce but some papers have reported that the formation of  
57  
58  
59  
60

1  
2  
3 ferritin oligomers can be ascribed to the reduction of disulphide bonds present on the  
4 surface of the protein monomers (while Fe(II) passes to Fe(III)).<sup>27</sup> The reactive thiol  
5 groups formed in this reduction would undergo subsequent S-S bridging (between several  
6 monomers) and so generating oligomeric ferritin structures. The formation of oligomeric  
7 structures was observed during the synthesis and increased by two-fold in just three hours  
8 (see supporting information).  
9  
10  
11  
12  
13  
14  
15

16  
17 Thus, in order to convert the ferritin oligomers into monomers, the originally  
18 synthesized product (see Figure 3 A) was treated with powerful reducing agents such as  
19 DTT (some authors have reported that the effectiveness of this reagent is dependent on its  
20 concentration<sup>20</sup> in such way that very high DTT concentrations are required to get a  
21 significant conversion of oligomers to monomers). In our experiments a 1% DTT  
22 treatment (see Figure 3B) did not produce the expected effect. Thus, the complex was also  
23 treated with 7 M guanidinium chloride (pH 3.5) which induces extensive unfolding of the  
24 protein and dissociation into subunits.<sup>20</sup> The results obtained indicated that the  
25 predominant reconstitution products from the oligomers are similar to ferritin monomers,  
26 as can be seen in Figure 3C. This chromatogram reveals also an important decrease in the  
27 sensitivity of the original protein peak (a factor of about 3-fold) which could be ascribed  
28 to a partial loss or degradation of the protein along the procedure. Guanidinium  
29 hydrochloride is a strong disruptive agent (commonly used for disrupting antigen-  
30 antibody binding) and the effect on proteins seems to be different depending on the  
31 protein target. Helical peptide studies show that guanidinium can be up to 4-fold more  
32 efficient than other reagents like urea when planar amino acid side chains are major  
33 contributors to helical stability according to some authors. In contrast, guanidinium is  
34 barely more efficient than urea if stabilization is due mainly to salt bridges.<sup>28</sup> However, no  
35 other significant species seem to be detected in the chromatogram after ultrafiltration. The  
36  
37  
38  
39  
40  
41  
42  
43  
44  
45  
46  
47  
48  
49  
50  
51  
52  
53  
54  
55  
56  
57  
58  
59  
60

1  
2  
3 guanidinium treated samples were stored for over a month and during this time no apparent  
4  
5 modification of the chromatographic profile was obtained (see supporting information).  
6  
7 Therefore, this preparation strategy was used for the final isotopically enriched species  
8  
9 synthesis as described in the procedures section.  
10

11  
12 Figure 4 shows the obtained chromatogram corresponding to the SEC-DF-ICP-MS  
13 separation of the isotopically enriched  $^{57}\text{Fe}$ -ferritin, monitoring  $^{56}\text{Fe}$  and  $^{57}\text{Fe}$ . As can be  
14  
15 seen, it is possible to address the presence of a pure peak containing mostly  $^{57}\text{Fe}$  (blue  
16  
17 trace) at the ferritin retention volume of 11.5 mL (comparable to that of the commercial  
18  
19 standard containing natural Fe in Fig. 2B). Some other Fe-containing species showing up  
20  
21 at 16 minutes, in the black trace, could be ascribed to some impurities present in the  
22  
23 commercial apo-ferritin standard and corresponding to other Fe-containing proteins (e.g.  
24  
25 transferrin). This assumption can be supported by the fact that the isotope abundance of  
26  
27 this peak corresponds to that of natural Fe and eluted at a different time than the  $^{57}\text{Fe}$ -  
28  
29 sought species.  
30  
31  
32  
33  
34  
35

### 36 **Characterization of the $^{57}\text{Fe}$ -ferritin tracer by SEC-ICP-MS and TEM**

37  
38  
39 Once the purity of the isotopically enriched ferritin standard was assessed, the Fe isotopic  
40  
41 composition of the enriched complex was calculated by injecting a triplicate of the  
42  
43 compound and monitoring all the isotopes (mass bias was taken into account) by MC-  
44  
45 ICP-MS. For data treatment, the linear regression slope approach was applied.<sup>29</sup>  
46  
47 According to these experiments, relative isotopic abundances of the synthetic  $^{57}\text{Fe}$ -ferritin  
48  
49 turned out to be:  $^{54}\text{Fe}$  0.08%,  $^{56}\text{Fe}$  3.9%,  $^{57}\text{Fe}$  92.6% and  $^{58}\text{Fe}$  3.5%. These values were  
50  
51 similar to the isotopic abundances of the Fe starting enriched material (95%  $^{57}\text{Fe}$ ) and  
52  
53 confirmed that the initial natural Fe present in the apo-ferritin was low while the  
54  
55 enrichment level with  $^{57}\text{Fe}$  is efficient using, Mohr's salt as a stable  $^{57}\text{Fe}(\text{II})$  source. In  
56  
57  
58  
59  
60

1  
2  
3 addition to the isotopic abundances, it is necessary to characterize the exact concentration  
4  
5 of the tracer in terms of Fe and protein concentration in order to address “the level of iron  
6  
7 saturation” of  $^{57}\text{Fe}$ -ferritin (meaning, the number of Fe atoms per ferritin molecule). In  
8  
9 that vein, a study was conducted by using post-column isotope dilution analysis after SEC  
10  
11 separation with ICP-MS detection as described in the procedures. By taking into account  
12  
13 the protein sequence from Swiss Prot database (this is, the number of S-containing amino  
14  
15 acids per subunit) and measuring the sulphur concentration in the protein using post-  
16  
17 column IDA, it is possible to transfer the obtained elemental concentration into ferritin  
18  
19 concentration. Simultaneously, standard natural Fe was used for quantification of  
20  
21 isotopically enriched  $^{57}\text{Fe}$  present in the synthesized standard (by reversed isotope dilution  
22  
23 analysis).  
24  
25  
26  
27

28 The use of post-column IDA for S and Fe determinations requires that protein  
29  
30 recovery through the column is quantitative. Since recoveries >85% have been obtained in  
31  
32 the used column for ferritin standards that requirement is secured. One further  
33  
34 consideration is the influence of the occurring H/L chains ratio variations in the ferritin  
35  
36 standards with respect to the amino acid composition predicted by the data bases. If the  
37  
38 differences are very high, this might result in an inaccuracy in the calculation of the  
39  
40 ferritin concentration (based on the S-containing amino acids). In order to check for this  
41  
42 possibility, a commercial human liver ferritin standard was analyzed simultaneously at  
43  
44 different concentrations by its S-content (using S-post column IDA with ICP-MS) as well  
45  
46 as by using a previously validated labelling immunoassay.<sup>24</sup> Both sets of experiments  
47  
48 (data not shown) provided undistinguishable results (slope of the plotted results 1.02 and  
49  
50 correlation coefficient  $r^2=0.992$ ) confirming the suitability, in this case, of the proposed  
51  
52 approach based on S measurement to address the protein concentration.  
53  
54  
55  
56  
57  
58  
59  
60



1  
2  
3 The obtained results for the characterization of the  $^{57}\text{Fe}$ -ferritin are summarized in  
4 Table 2 including protein concentration, Fe concentration and Fe:ferritin ratios. As  
5 average, the number of Fe atoms per ferritin turned out to be about 2200 which is in good  
6 agreement with the existing literature on this regard. This documents that even when the  
7 protein cage can accommodate up to 4500 atoms of Fe, naturally found Fe:ferritin ratios  
8 are lower and do not exceed 1500 atoms/molecule of ferritin in liver cells of  
9 haemochromatosis patients.<sup>30</sup>  
10  
11  
12  
13  
14  
15  
16  
17  
18

19 To finally confirm that is  $^{57}\text{Fe}$  is specifically incorporated into the ferritin cage and  
20 not bound unspecifically within the protein, TEM images of the apoferritin, commercial  
21 holoferitin and the synthesized  $^{57}\text{Fe}$ -ferritin were taken for comparative purposes. Figure  
22 5 shows all the images together with the histograms corresponding to the mean diameters  
23 determined in each case. Thus, mean diameters were  $3.8 \pm 1.0$ ,  $5.80 \pm 0.85$  and  $6.82 \pm$   
24  $0.70$  nm for apoferritin, commercial holoferitin and synthesized  $^{57}\text{Fe}$ -ferritin. These  
25 results corroborate that the synthesis used in this work has successfully accomplished the  
26 formation of iron oxide nanoparticles into the core of apoferritin. Additionally, the size of  
27 the Fe core seems higher in the synthesized protein than in the case of the commercial  
28 holoferitin (5.80 vs. 6.82). In order to quantitatively address these differences in terms of  
29 the Fe content of the different ferritin forms, the synthesized  $^{57}\text{Fe}$ -ferritin was used as  
30 tracer to conduct species specific isotope dilution analysis for the determination of the Fe  
31 content in the commercial apo and holoferitin using the methodology we described  
32 previously in the literature.<sup>31</sup> Figure 6 shows the chromatograms obtained for apoferritin  
33 (Figure 6A, low Fe content) and for holoferitin (Figure 6B, containing a higher Fe  
34 concentration) both from horse spleen after mixing with the synthesized tracer and IDA  
35 analysis.  
36  
37  
38  
39  
40  
41  
42  
43  
44  
45  
46  
47  
48  
49  
50  
51  
52  
53  
54  
55  
56  
57  
58  
59  
60

1  
2  
3 Table 3 shows a summary of the obtained results for these determinations (total  
4 protein concentration was calculated by conducting post-column isotope dilution of S as  
5 previously described). It can be observed that the Fe:ferritin ratios in the apo-ferritin from  
6 horse spleen are very low (about 200) but there is still some Fe present in the protein core,  
7 as observed in the TEM image. On the other hand, the Fe:ferritin content in the  
8 commercial horse spleen ferritin turned out to be about 1000 atoms/molecule ferritin that  
9 is remarkably lower (by a factor of 2-fold) than in the synthesized ferritin and also in  
10 agreement with the TEM image (revealing an Fe core of about 5.8) and with the reported  
11 values in the literature.<sup>32</sup> In brief, after such characterization results it can be concluded  
12 that the synthesized <sup>57</sup>Fe-ferritin standard can be used as a nanometabolic tracer for  
13 quantitative studies, for instance, on the Fe release or its incorporation kinetics under  
14 different pathological situations and be compared with normal healthy conditions.  
15  
16  
17  
18  
19  
20  
21  
22  
23  
24  
25  
26  
27  
28  
29

### 30 **Determination of Fe:ferritin ratios in serum samples.**

31  
32  
33 The labeled ferritin was applied for the quantification of ferritin-bound iron in different  
34 human serum samples (n=8) as described in the procedures section. In Table 4 the  
35 determined ferritin-bound iron concentrations are represented. Here, a mean concentration  
36 of  $12.35 \pm 6.99$  ng g<sup>-1</sup> ferritin-bound iron was determined which is in excellent agreement  
37 to previously obtained results using post column IDA after protein purification.<sup>24</sup> To  
38 address the serum ferritin concentration, each serum sample was analyzed by ECLIA  
39 enabling the calculation of the Fe:ferritin ratios. The obtained Fe:ferritin ratios indicate a  
40 correlation between low serum ferritin concentration (<75 ng mL<sup>-1</sup>) and higher Fe:ferritin  
41 ratios, similarly to what was observed in previous experiments with this kind of samples.  
42  
43  
44  
45  
46  
47  
48  
49  
50  
51  
52  
53  
54  
55  
56  
57  
58  
59  
60

1  
2  
3 previously described).<sup>24</sup> Consequently, no sample recoveries during purification or  
4  
5 chromatographic separation have to be taken into account.  
6  
7

## 8 **Conclusions**

9  
10  
11 The chemical incorporation of Fe(II) from dissolved  $(\text{NH}_4)_2\text{Fe}(\text{II})(\text{SO}_4)_2$  into apo-ferritin  
12  
13 has proved to follow a first order reaction kinetics catalyzed by apo-ferritin. Importantly,  
14  
15 during the Fe(II) incorporation into the protein the formation of ferritin oligomers was  
16  
17 observed. To disrupt such aggregates, 7 M guanidinium hydrochloride (pH 3.5) produced  
18  
19 satisfactory results and showed that the interactions to form oligomers are relatively  
20  
21 strong. The studied and optimized synthesis was then conducted with isotopically  
22  
23 enriched  $(\text{NH}_4)_2^{57}\text{Fe}(\text{II})(\text{SO}_4)_2$  and the resulting isotopically enriched protein turned out to  
24  
25 provide Fe:ferritin ratios of about 2200 Fe atoms per ferritin and about  $^{57}\text{Fe}$  92.6%  
26  
27 isotopic abundances as obtained by MC-ICP-MS.  
28  
29  
30  
31  
32

33 The complementary information about NPs size provided by the TEM  
34  
35 measurement in the same standards revealed first, that the  $^{57}\text{Fe}$  is incorporated specifically  
36  
37 within the protein core in the form of an iron oxide nanoparticle with a final diameter of  
38  
39 about 6.8 nm; second, the use of the synthesized nanotracer of  $^{57}\text{Fe}$ -ferritin with SEC-ICP-  
40  
41 MS provided important information on the saturation level of the commercial horse spleen  
42  
43 ferritin in the apo and holo forms and their correlation with the inner protein core size  
44  
45 variation obtained by TEM. Therefore, the developed enriched standard together with the  
46  
47 optimized methodology has been applied to address Fe:ferritin ratios in important  
48  
49 biological samples (e.g. serum) and will be applied in other samples to understand a bit  
50  
51 further the implication of ferritin and iron uptake in health and disease (e.g.  
52  
53 hyperferritinemias which may be associated to iron overload, inflammation or even  
54  
55 cancer).<sup>33</sup> In addition, the proposed strategy could have a great impact to investigate in  
56  
57  
58  
59  
60

1  
2  
3 depth the efficacy of new Fe-pharmaceutical preparations to combat Fe deficiencies (e.g.  
4  
5 those using Fe-nanoparticles, recently applied to treat severe anaemia).<sup>34</sup>  
6  
7

## 8 9 **Acknowledgements**

10  
11 The authors want to thank Prof. Santiago García-Granda for his help on the X-ray  
12  
13 characterization of the synthesized Mohr's salt and Prof. Nacho Garcia Alonso for the  
14  
15 help with the MC-ICP-MS experiments. The financial support from MICINN through the  
16  
17 FPU grant AP2008-04449 of T. Konz and through the projects CTQ2006-02309 and  
18  
19 CTQ2011-23038 is gratefully acknowledged.  
20  
21  
22  
23

## 24 25 **References**

- 26  
27  
28 <sup>1</sup> M. Wessling-Resnick, *Annu. Rev. Nutr.*, 2000, **20**, 129-151.  
29  
30 <sup>2</sup> N. C. Andrews, *N. Engl. J. Med.*, 1999, **341**, 718-724.  
31  
32 <sup>3</sup> M. Muñoz, J. A. García-Erce, A. F. Remacha. *J. Clin. Pathol.*, 2011, **64**, 287-296.  
33  
34 <sup>4</sup> H. A. Huebers, M. J. Eng, B. M. Josephson, N. Ekpoom, R. L. Rettmer, R. F. Labbé, P. Pootrakul, C. A  
35  
36 Finch. *Clin. Chem.* 1987, **33**, 273-277.  
37  
38 <sup>5</sup> M. E. Del Castillo Busto, M. Montes-Bayón, J. Bettmer, A. Sanz-Medel, *Analyst*, 2008, **133**, 379-384  
39  
40 <sup>6</sup> M. A. Knovich, J. A. Storey, L. G. Coffman, S. V. Torti, F. M. Torti. *Blood Reviews* 2009, **23**, 95-104.  
41  
42 <sup>7</sup> E. C. Theil, *J. Nutr.* 2003, **133**, 1549S-1553S  
43  
44 <sup>8</sup> S. Ferraro, R. Mozzi, M. Panteghini. *Clin. Chem. Lab. Med.* 2012, **50**, 1911-1916.  
45  
46 <sup>9</sup> F. Carmona, O. Palácios, N. Gálveza, R. Cuesta, S. Atriand, M. Capdevila, J. M. Domínguez-Vera. *Coord.*  
47  
48 *Chem. Rev.*, 2013, **257**, 2752-2764.  
49  
50 <sup>10</sup> S. Stanley. *Current Op. Biotech.*, 2014, **28**, 69-74  
51  
52 <sup>11</sup> N. D. Chasteen, P. M. Harrison. *J. Struct. Biol.*, 1999, **126**, 182-194.  
53  
54 <sup>12</sup> M. Wagstaff, M. Worwood, A. Jacobs, *Biochem. J.* 1978, **173**, 969-977.  
55  
56 <sup>13</sup> L. Zecca, M. B. H. Youdim, P. Riederer, J. R. Connor, R. R. Crichton. *Nature Rev. Neurosci.*, 2004, **5**,  
57  
58 863-873.  
59  
60 <sup>14</sup> Y. Ke, Z. M. Qian. *Lancet Neurol.*, 2003, **2**, 243-253.  
<sup>15</sup> D. B. Kell, E. Pretorius. *Metallomics*, 2014, **26**, 748-773  
<sup>16</sup> M. Hoppler, L. Meile, T. Walczyk. *Anal. Bioanal. Chem.* 2008, **390**, 53-59.  
<sup>17</sup> M. Hoppler, C. Zeder, T. Walczyk. *Anal. Chem.* 2009, **81**, 7368-7372.  
<sup>18</sup> J. A. Rodríguez-Castrillón, M. Moldovan, J. I. García Alonso, J. J. Lucena, M. L. García-Tomé, L.  
Hernández-Apaolaz. *Anal. Bioanal. Chem.* 2008, **390**, 579-590

- 1  
2  
3  
4  
5  
6  
7  
8  
9  
10  
11  
12  
13  
14  
15  
16  
17  
18  
19  
20  
21  
22  
23  
24  
25  
26  
27  
28  
29  
30  
31  
32  
33  
34  
35  
36  
37  
38  
39  
40  
41  
42  
43  
44  
45  
46  
47  
48  
49  
50  
51  
52  
53  
54  
55  
56  
57  
58  
59  
60
- 
- <sup>19</sup> D. De Silva, D. M. Miller, D. W. Reif, S. D. *Arch. Biochem. Biophys.* 1992, **293**, 409-415.
- <sup>20</sup> Y. Niitsu, I. Listowsky I. *Biochemistry* 1973, **12**, 4690-4694.
- <sup>21</sup> M. Wang, W. Feng, W. Lu, B. Li, B. Wang, M. Zhu, Y. Wang, H. Yuan, Y. Zhao, Z. Chai. *Anal. Chem.*, 2007, **79**, 9128–9134.
- <sup>22</sup> C. Rappel, D. Schaumlöffel. *Anal. Bioanal. Chem.*, 2008, **390**, 605–615.
- <sup>23</sup> N. Zinn, R. Krüger, P. Leonhard, J. Bettmer. *Anal. Bioanal. Chem.*, 2008, **391**, 537–543
- <sup>24</sup> T. Konz, E. Añón-Alvarez, M. Montes-Bayon, A. Sanz-Medel. *Anal. Chem.*, 2013, **85**, 8334–8340.
- <sup>25</sup> K. G. Heumann, L. Rottmann, J. Vogl, *J. Anal. At. Spectrom.*, 1994, **9**, 1351-1355.
- <sup>26</sup> G. R. Bakker, R.F. Boyer. *J. Biol. Chem.*, 1986, **261**, 13182-13185.
- <sup>27</sup> M. Wagstaff, M. Worwood, A. Jacobs. *Biochem. J.* 1978, **173**, 969-77
- <sup>28</sup> W. K. Lim, J. Rosgen, S. W. Englander. *PNAS*, 2009, **106**, 2595
- <sup>29</sup> V. N. Epov, S. Beraïl, M. Jimenez-Moreno, V. Perrot, C. Pecheyran, D. Amouroux, O. F. X. Donard. *Anal. Chem.*, 2010, **82**, 5652-62.
- <sup>30</sup> Y. H. Pan, K. Sader, J. J. Powell, A. Bleloch, M. Gass, J. Trinick, A. Warley, A. Li, R. Brydson, A. Brown. *J. Struct. Biol.*, 2009, **166**, 22–31.
- <sup>31</sup> M. E. Del Castillo Busto, M. Montes-Bayon, A. Sanz-Medel. *Anal. Chem.*, 2006, **78**, 8218-8226.
- <sup>32</sup> S. Gider, D. Awschalom, T. Douglas, S. Mann, M. Chaparala. *Science*, 1995, **268**, 77–80.
- <sup>33</sup> S. I. Shpyleva, V. P. Tryndyak, O. Kovalchuk, A. Starlard-Davenport, V. F. Chekhun, F. A. Beland, I. P. Pogribny, *Breast Cancer Res. Treat.* 2011, **126**, 63–71.
- <sup>34</sup> M. R. Jahn, H. B. Andreasen, S. Fütterer, T. Nawroth, V. Schünemann, U. Kolb, W. Hofmeister, M. Muñoz, K. Bock, M. Meldel, P. Lagguth. *Eur. J. Pharm. Biopharm.*, 2011, **78**, 480-91.

**Table 1.** Instrumental operating conditions for Fe and S measurements in ferritin.

<b>Thermo Element 2</b>	
RF Power	1350 W
Mass Resolution R	4000 (medium resolution)
Isotopes monitored	$^{56}\text{Fe}$ , $^{57}\text{Fe}$ , $^{32}\text{S}$ , $^{34}\text{S}$
Nebulizer	Concentric
Spray chamber	Scott-double pass, 21°C
Cooling gas	15.5 L min <sup>-1</sup>
Auxiliary gas	0.90 L min <sup>-1</sup>
Sample gas	0.90 L min <sup>-1</sup>
<b>HPLC devices and parameter</b>	
HPLC device for UV/Vis	<b>Agilent 1100 series</b>
HPLC device for ICP-MS	<b>Shimadzu LC-20AD</b>
Flow rate	0.75 ml min <sup>-1</sup>
Mobile phase	50 mM ammonium acetate (pH 7.4)
Chromatographic column	Superdex 200 10/300 GL

**Table 2.** Quantitative results obtained for the analysis of total ferritin, iron in ferritin and Fe:ferritin ratio in the synthesized isotopically enriched  $^{57}\text{Fe}$ -ferritin.

	<b>Average</b>	<b>SD</b>	<b>%RSD</b>
<b>Fe concentration</b>	2.86 $\mu\text{g mL}^{-1}$	0.04	1.46
	51.58 $\text{nmol mL}^{-1}$	0.76	
<b>Ferritin concentration</b>	13.5 $\mu\text{g mL}^{-1}$	1.32	9.8
	23.4 $\text{pmol mL}^{-1}$	2.29	
<b>Fe:Ferritin</b>	<b>2213</b>	185	8.4

**Table 3.** Quantitative results obtained for the analysis of total ferritin, iron and Fe:ferritin ratios in the quantified commercially available ferritin standards.

	Horse-spleen (n=3)	Apo-ferritin
<b>Fe concentration</b>	1.47 ppm	6.7 ppm
	26.2 $\mu\text{mol/L}$	119.5 $\mu\text{mol/L}$
<b>Ferritin concentration</b>	14.3 ppm	311.7 ppm
	26.2 nmol/L	623.2 nmol/L
<b>Fe:Ferritin</b>	<b>1030 <math>\pm</math> 20</b>	<b>190</b>

**Table 4.** Quantitative results obtained for the analysis of total ferritin, iron and Fe:ferritin ratios in serum samples from patients containing ferritin levels below 75 ng mL<sup>-1</sup>.

<b>Fe (SEC-DF-ICP-MS)</b>		<b>Ferritin (ECLIA)</b>		<b>Fe:Ferritin</b>
ng g <sup>-1</sup>	nmol g <sup>-1</sup>	ng ml <sup>-1</sup>	fmol ml <sup>-1</sup>	
2.65	0.05	9	17.18	2766
11.17	0.20	73	139.37	1436
12.16	0.22	33	63.01	3456
12.23	0.22	27	51.55	4249
15.99	0.29	60	114.55	2500
17.45	0.31	54	103.10	3031
23.66	0.42	67	127.92	3312



---

## Legends of Figures

**Figure 1.** Incorporation kinetics using 1  $\mu$ M apo-ferritin solution incubated with 0 to 10 mM of  $(\text{NH}_4)_2^{57}\text{Fe}(\text{II})(\text{SO}_4)_2$  as Fe(II) source. Variation of the absorbance detected at 380 nm.

**Figure 2.** Size exclusion chromatogram of **A)** the reaction products of the incubation of apo-ferritin with  $(\text{NH}_4)_2^{57}\text{Fe}(\text{II})(\text{SO}_4)_2$  using UV/VIS detection (monitoring the signals at 280 and 380 nm) and **B)** Chromatogram of the commercial standard of Fe-containing ferritin from horse spleen using the same column.

**Figure 3.** Chromatograms obtained by UV/Vis detection: **A)** directly after apo-ferritin loading with Fe(II) and after the reaction products is treated with **B)** 1% DTT, **C)** 7 M guanidinium chloride (pH 3.5). Monomer eluting at about 11.5 mL and oligomers at 8 mL.

**Figure 4.** Chromatogram corresponding to the SEC-DF-ICP-MS separation of the isotopically enriched  $^{57}\text{Fe}$ -ferritin complex monitoring  $^{56}\text{Fe}$  and  $^{57}\text{Fe}$  (black and blue trace, respectively) at about 10.5 mL.

**Figure 5.** Images obtained by TEM of the different ferritins from horse spleen together with the histograms of the measured nanoparticle diameters: **A)** apoferritin, **B)** holoferritin and **C)**  $^{57}\text{Fe}$ -ferritin synthesized with the proposed methodology.

**Figure 6.** Size exclusion chromatograms obtained from a mixture of the synthesized isotopically enriched  $^{57}\text{Fe}$ -ferritin and **A)** apo-ferritin (equine spleen) **B)** human spleen ferritin by using the  $^{57}\text{Fe}$ -ferritin tracer by using DF-ICP-MS detection both eluting at about 10.5 mL.

1  
2  
3  
4  
5  
6  
7  
8  
9  
10  
11  
12  
13  
14  
15  
16  
17  
18  
19  
20  
21  
22  
23  
24  
25  
26  
27  
28  
29  
30  
31  
32  
33  
34  
35  
36  
37  
38  
39  
40  
41  
42  
43  
44  
45  
46  
47  
48  
49  
50  
51  
52  
53  
54  
55  
56  
57  
58  
59  
60

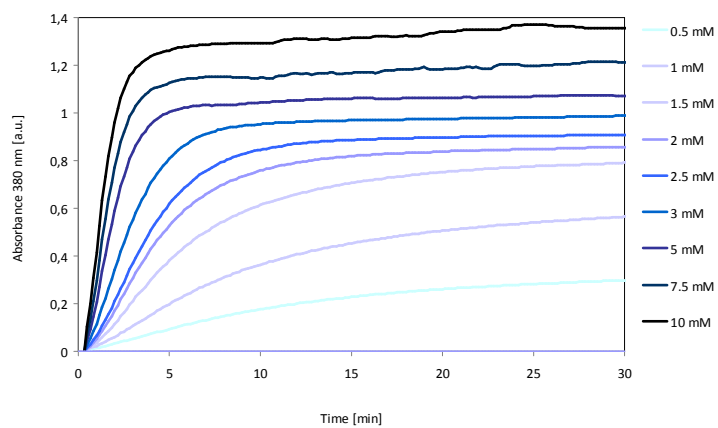
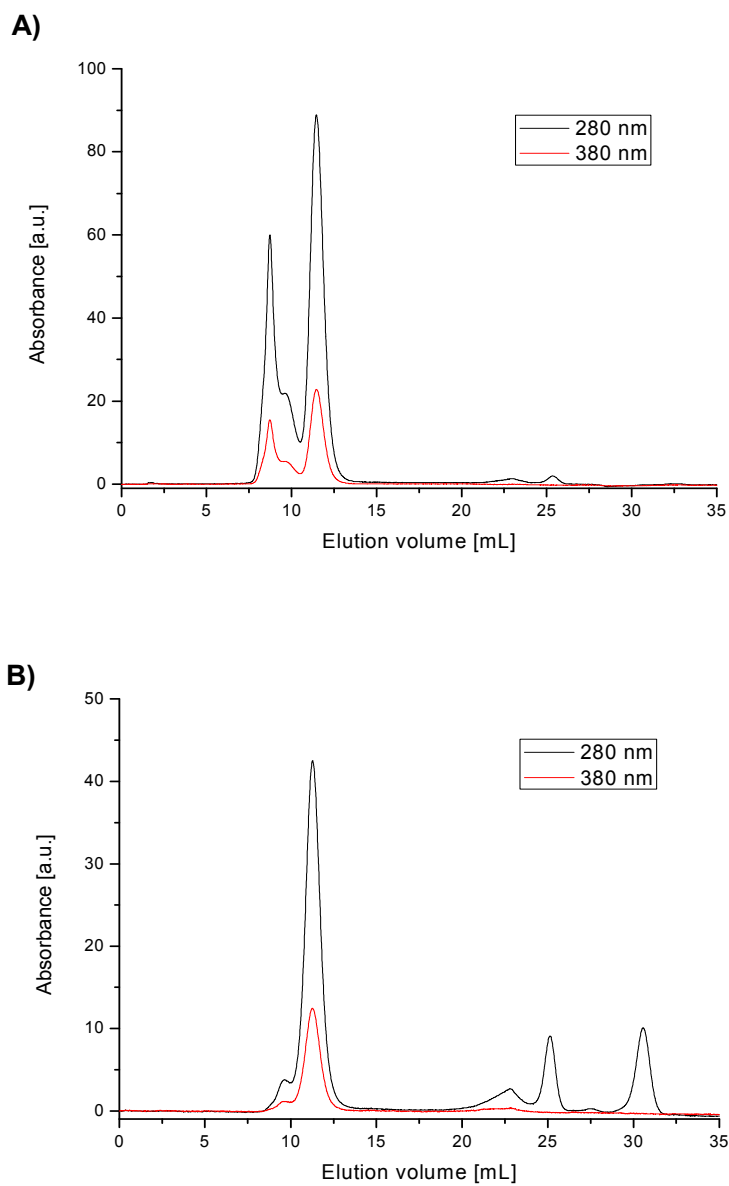


Figure 1



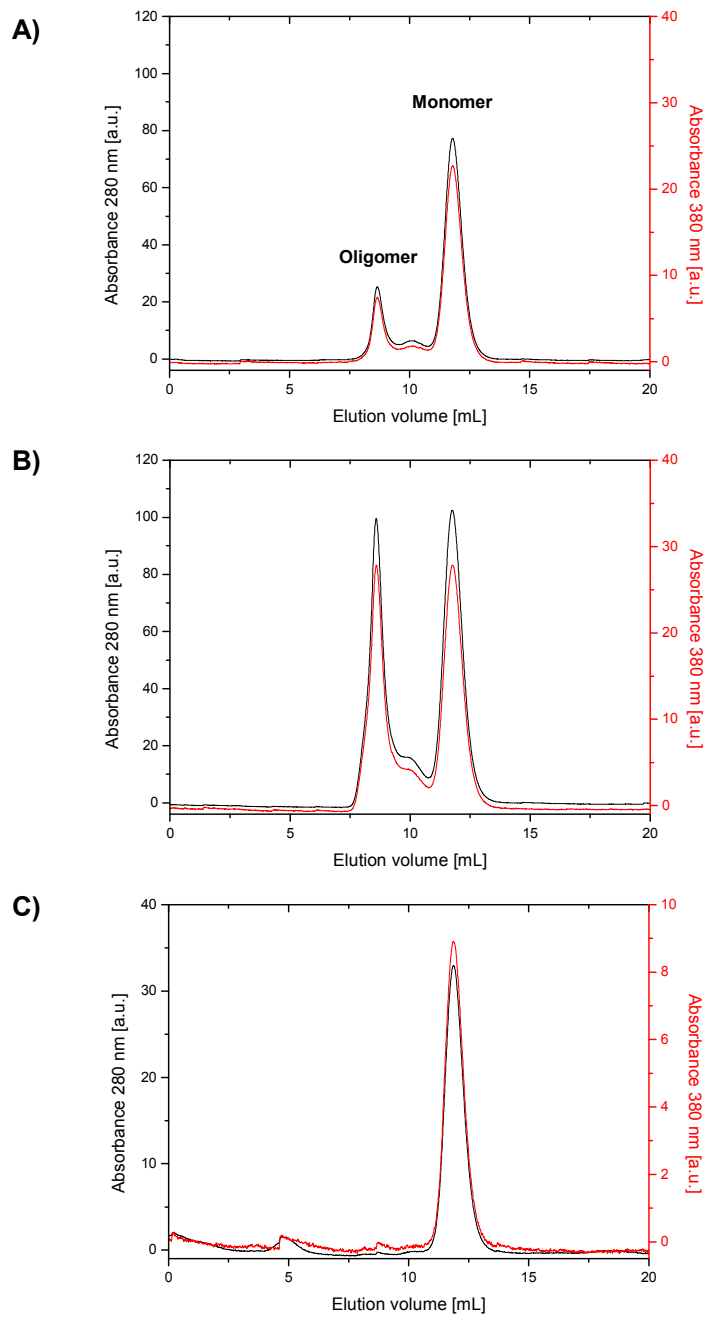


Figure 3

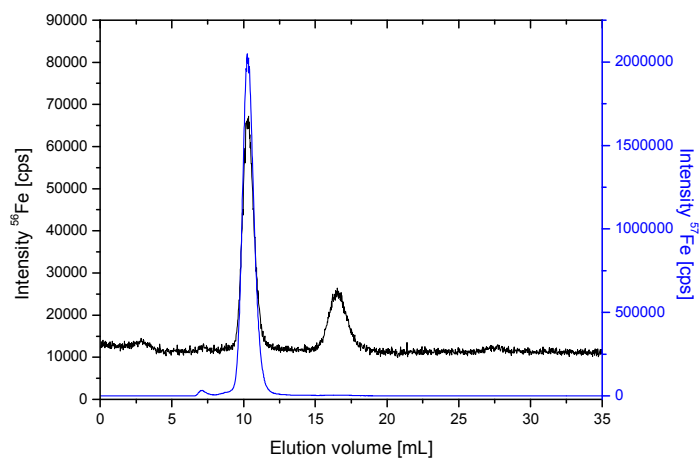


Figure 4

1  
2  
3  
4  
5  
6  
7  
8  
9  
10  
11  
12  
13  
14  
15  
16  
17  
18  
19  
20  
21  
22  
23  
24  
25  
26  
27  
28  
29  
30  
31  
32  
33  
34  
35  
36  
37  
38  
39  
40  
41  
42  
43  
44  
45  
46  
47  
48  
49  
50  
51  
52  
53  
54  
55  
56  
57  
58  
59  
60

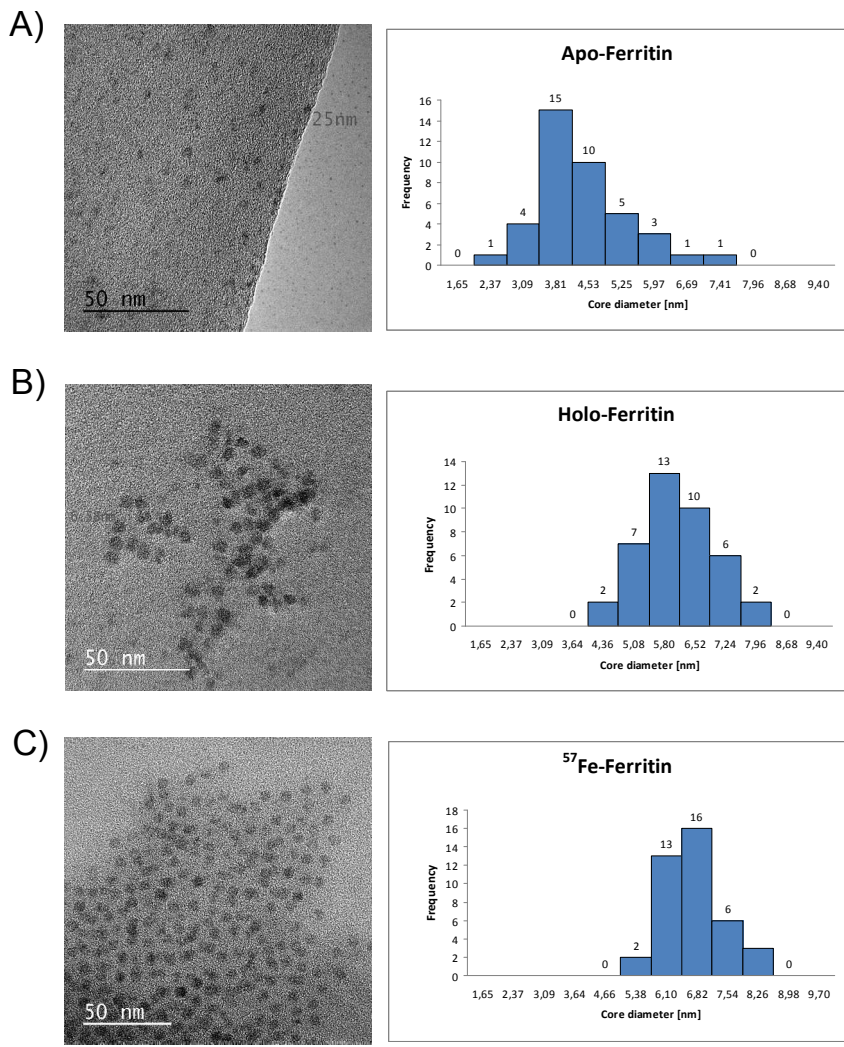


Figure 5

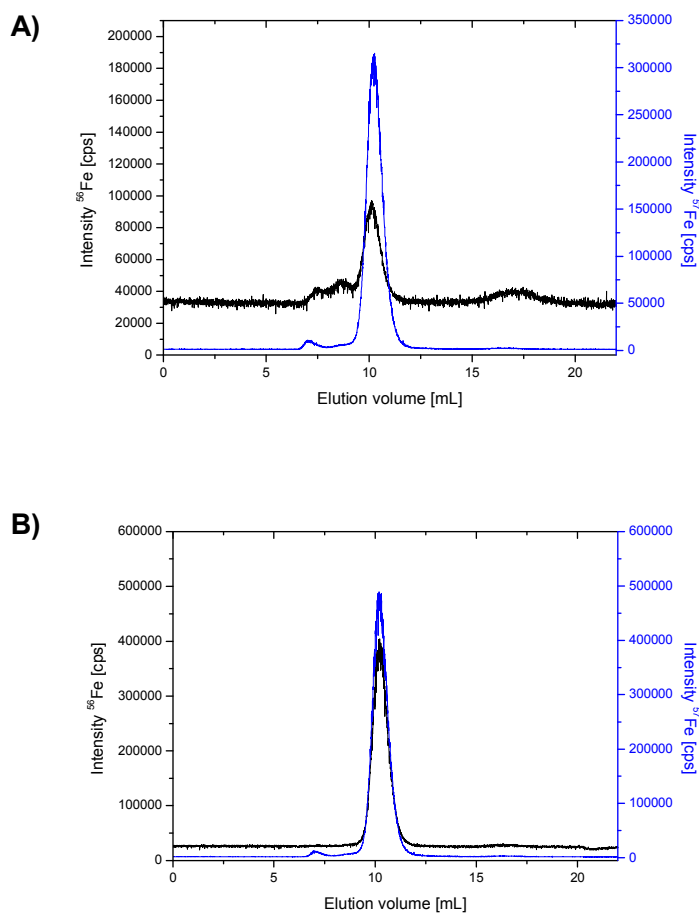


Figure 6